Clutter Effect on the Guidance of a Semi-Active Radar Homing Missile

Susumu Miwa* and Fumiaki Imado†
Mitsubishi Electric Corporation, Tokyo, Japan

A method of simulating clutter spectrum in a semi-active radar homing missile is introduced. The results of the simulation are shown for various cases such as look down, equal altitude, look up and spirally descending target. It is made clear that the low altitude as well as the look down gives a main lobe clutter high enough to mask the target if the target maneuvers with an appropriate lateral acceleration. Conditions in which this masking effect occur are considered and verified by simulation. The results show that the missile effective zone is greatly affected by the main lobe clutter. A guidance concept to avoid this effect is suggested.

Nomenclature

a = lateral acceleration
$\boldsymbol{a}$ = unit vector of dS-A
A = aircraft with transmitter
d = duty cycle
dP = clutter power due to dS
ds = small area on the Earth
D = distance along X axis
f_{dc} = Doppler frequency of clutter
f_{dt} = Doppler frequency of target
F_0 = transmitter frequency
G_A = transmitter antenna gain toward dS
G_{AMAX} = maximum transmitter antenna gain
G_M = receiver antenna gain toward dS
G_{MMAX} = maximum receiver antenna gain
h = altitude
$\boldsymbol{m}$ = unit vector of dS-M
M = missile with receiver
$\boldsymbol{p}$ = vector sum of $\boldsymbol{a}$ and $\boldsymbol{m}$
P_t = transmitter power (center line power for pulsed Doppler radar, average power for continuous wave)
P_{tgt} = signal power reflected by target
r = radius of gyration
R_A = distance between aircraft and dS
R_{AT} = distance between aircraft and target
R_M = distance between missile and dS
R_{TM} = distance between target and missile
T = target
v = velocity
X, Y = coordinates in a plane
α = angle between LOS and v_t
Δf = Doppler frequency difference
ϵ_A = angle between A-T and A-dS
ϵ_M = angle between M-T and M-dS
θ = angle to define dS
λ = wavelength
σ^0_{AM} = bistatic scattering coefficient of dS
σ_T = radar cross section of target
Φ = angle of gyration
Φ_{AM} = angle between v_a and A-M
Φ_{MA} = angle between v_m and A-M
Ψ_A = angle between v_a and A-dS
Ψ_{AT} = angle between v_a and A-T
Ψ_M = angle between v_m and M-dS
Ψ_{MT} = angle between v_m and T-M
Ψ_{TA} = angle between v_t and A-T
Ψ_{TM} = angle between v_t and T-M
$( )'$ = time derivative
$( )_0$ = initial value
$( )_{1 \text{ or } 2}$ = values in Example 1 or 2
$( )_a$ = denotes aircraft
$( )_m$ = denotes missile
$( )_t$ = denotes target

Received June 20, 1985; revision received Jan. 2, 1986.

*Manager, Information Network Systems Development, Headquarters.
†Chief Engineer, Mechanical Systems and Technology Department, Central Research Laboratory. Member AIAA.

Introduction

A METHOD of calculating clutter spectrum in a semi-active radar homing missile, combining the bistatic radar equation and a flight simulation program, GPMS[1] (General Purpose Tactical Missile Simulation Program), is derived and the main lobe clutter is shown to exceed the target signal level in the case of look down.[2] The target Doppler frequency coincides with the main lobe clutter frequency when the target velocity vector comes close to perpendicular to the line of sight (LOS). It is, therefore, easily assumed that if the target maneuvers with a large lateral acceleration at low altitude, it may have a chance to be masked by the main lobe clutter.

It may be worth while to make clear in what case the main lobe clutter level exceeds the target level and how the effect reduces the missile effective zone. It may also be necessary to take some countermeasure when this effect is detrimental to the missile performance. In this paper, these problems are handled after reviewing the clutter simulation method.

Method of Clutter Spectrum Simulation

Figure 1 shows the relative positions of an aircraft, a missile, and a target, and designation of variables necessary for calculations. The aircraft flying at a speed of v_a carries a transmitter with the antenna radiating the energy mainly to the target, but partly to the other directions due to the side lobes. The missile with a speed of v_m, has a receiver antenna that directs the target but also receives clutter through the side lobes.

The clutter power due to a small radiated portion on the dS is expressed by

$$dP = \frac{(P_t/d^2)\lambda^2 G_A G_M \sigma^0_{AM} dS}{(4\pi)^3 R_A^2 R_M^2} \tag{1}$$

The following assumptions are made to perform this calculation. The radar system is either CW or pulsed Doppler. In the latter case, the PRF (pulse recurrence frequency) is higher than the highest target Doppler frequency so that no frequency ambiguity occurs. The antenna patterns of the transmitter and receiver are rotatory symmetrical to the antenna axis. G_A and G_M then become functions of ϵ_A and ϵ_M, respectively. The bistatic scattering coefficient, representing the scattering coefficient coming from A and going to M at dS, is equal to a monostatic scattering coefficient to the direction of p, which is a vector sum of unit vectors a and m[3]. Effect of curvature of the Earth is neglected because the distance handled is less than a few tens of kilometers.

The small area dS is selected as follows. The equal range surface of the clutter path ($R = R_A + R_M = \text{const}$) forms an ellipsoid of revolution with the aircraft and the missile at its focuses. Its intersection with the Earth's surface forms an ellipse. The increment of R forms another ellipse with its center slightly shifted. The dS is selected dividing the area between these two ellipses with the angle $d\theta$ as shown in Fig. 2. In this method the radiated area on the Earth is easily distinguished from the non-radiated area in the case of the pulsed Doppler radar.

The dP has a Doppler shifted frequency as shown in Eq. (2).

$$f_{dc} \approx \left\{F_0 + \frac{1}{\lambda}(v_a \cos\Psi_A + v_m \cos\Psi_M)\right\} - \left\{F_0 + \frac{1}{\lambda}(v_a \cos\Phi_{AM} - v_m \cos\Phi_{MA})\right\} \quad (2)$$

The first term represents the Doppler-shifted F_0 due to the reflection at dS while the second term is that of the direct transmission to the receiver. Values such as v_a, v_m, Φ_{AM}, and Φ_{MA} can be derived from the GPMS, which calculates all the necessary flight data of the aircraft, missile, and target.

In order to obtain a clutter frequency spectrum, all dP of the related area are distributed to the corresponding frequency region and summarized. Combining GPMS with Eqs. (1) and (2), the spectrum is drawn at an arbitrary time interval.

The target signal P_{tgt} and its Doppler frequency f_{dt} are calculated by Eqs. (3) and (4).

$$P_{tgt} = \frac{P_t \lambda^2 G_{AMAX} G_{MMAX} \sigma_t}{(4\pi)^3 R_{AT}^2 R_{TM}^2} \quad (3)$$

$$f_{dt} \approx \left\{F_0 + \frac{1}{\lambda}(v_a \cos\Psi_{AT} + v_t \cos\Psi_{TA} + v_t \cos\Psi_{TM} + v_m \cos\Psi_{MT})\right\} - \left\{F_0 + \frac{1}{\lambda}(v_a \cos\Phi_{AM} - v_m \cos\Phi_{MA})\right\} \quad (4)$$

The first term of Eq. (4) is the Doppler shifted F_0 due to the reflection by the target. The reason the second term is subtracted in Eqs. (2) and (4) is due to the receiver mechanism. If the aircraft, missile, and target are nearly in line, f_{dt} becomes $(2/\lambda)(v_m + v_t)$ which is proportional to the relative speed between the missile and target. The target Doppler spectrum is easily added to the clutter spectrum.

Clutter Simulation Results

Parameters

Simulations are conducted using the following parameters.

Transmitter: Radar type = pulsed Doppler; $P_t = 750$ W; $d = 0.5$; $PRF = 300$ kHz; wavelength = 3 cm (10 GHz).

Antenna directivity pattern: Antenna directivity patterns are calculated by assuming the current distribution to be Taylor's. Figure 3 shows the patterns of the transmitter and receiver antenna.

Scattering coefficient: There are fairly abundant data on the monostatic scattering coefficient.[4] We chose Fig. 4 as a

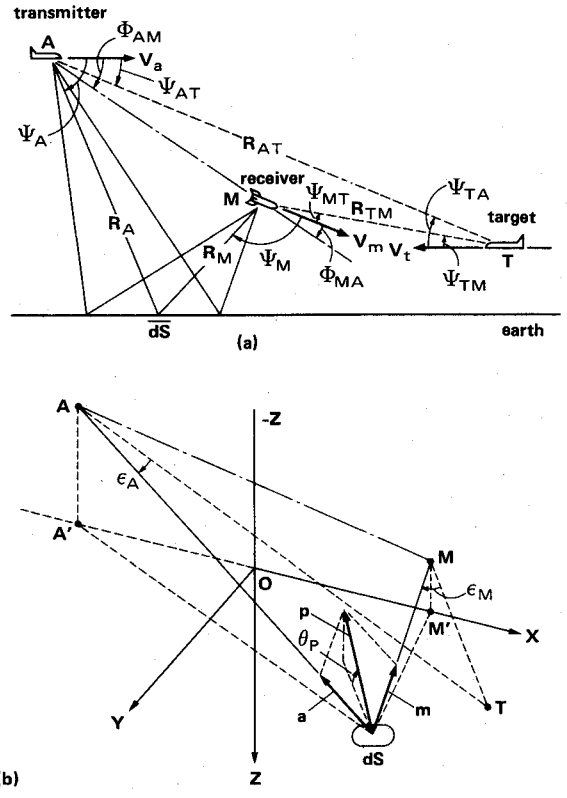

Fig. 1 Geometry and designation of variables, a) side view, b) bird's-eye view.

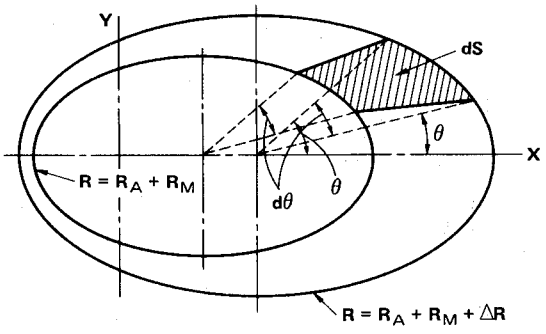

Fig. 2 Selection of dS.

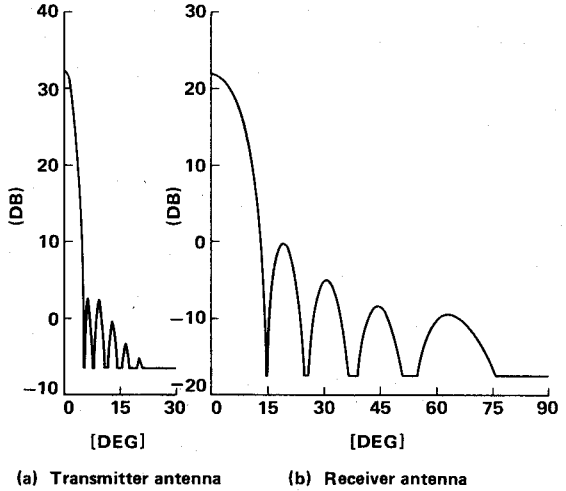

(a) Transmitter antenna **(b) Receiver antenna**

Fig. 3 Antenna directivity patterns.

reference which corresponds to the lowest line of "Vertical polarization, city (scattering coefficient on the city environment by vertical polarization)" in Ref. 4.

Target radar cross section: Target radar cross section is assumed to be 8 m^2, ignoring the change due to its aspect angle.

Look Down Case

First, a simulation for the look down case is performed under the following conditions. An aircraft flies toward a predicted intercept point with an initial altitude of 1200 m, at a constant speed of 300 m/s. A target, which is assumed to be a constant speed mass point, flies horizontally at an altitude of 300 m, and its initial velocity (300 m/s) vector is opposite the aircraft. It begins to turn with a lateral acceleration of 5 g as a missile is fired from the aircraft at a horizontal distance of 7500 m.

A missile, which is a typical but hypothetical air-to-air type with a two-stage, 12.5-s total thrust time rocket rotor, pursues the target with the proportional navigation law. The trajectories of the aircraft, target, and missile are drawn in Fig. 5.

The clutter power spectra in the missile receiver from 1 s after firing through 9 s are shown in Fig. 6. The following data are derived from this figure: the main lobe clutter is seen at the highest frequency of the clutter, and the level exceeds the target signal; side lobe clutter is fairly flat and the level is higher than the thermal noise (−139 dBm/kHz for a noise figure of 5 dB) but lower than the target signal; the target Doppler frequency is far separate from the clutter at initial phase but gradually comes close and is covered by the main lobe clutter at 8 s (this is caused by the target's constant 5-g maneuver); if the target signal is covered by the main lobe clutter, the missile loses tracking capability unless some countermeasure is taken. Figure 6 is drawn assuming the relock is assured.

Equal Altitude Case

Second, the equal altitude case is investigated. Conditions are the same as the look down case, except that the aircraft, missile and target always fly at a specified altitude. Table 1 shows the main and side lobe clutter levels at 5 s after firing, the target signal level at this time being −90 dBm.

The main lobe clutter is lower than the signal at altitudes of 10,000 and 6000 m; however, it becomes higher at 1200 m. This trend continues for 300 and 100 m, giving almost the same main lobe clutter level as the look down case.

Look Up Case

Third, the case is checked where the target altitude is higher than the aircraft. Again, conditions are the same as previous cases except the 300-m initial altitude of the aircraft and the target altitude. The clutter levels at 5 s after firing are summarized in Table 2, the target signal level being approximately −91 dBm.

In the case where the aircraft looks up at targets in altitudes of 3600 and 1800 m, the main lobe clutter can not be seen at all. In the case of 300 m vs 1200 m, a small sign of the main lobe clutter is seen but the level is still almost the same as the side lobe clutter. It may be admitted that no main lobe clutter effect is seen in the look up case if there is any appreciable look up angle.

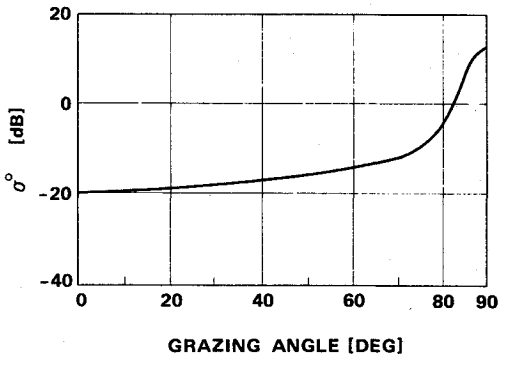

Fig. 4 Scattering coefficient.

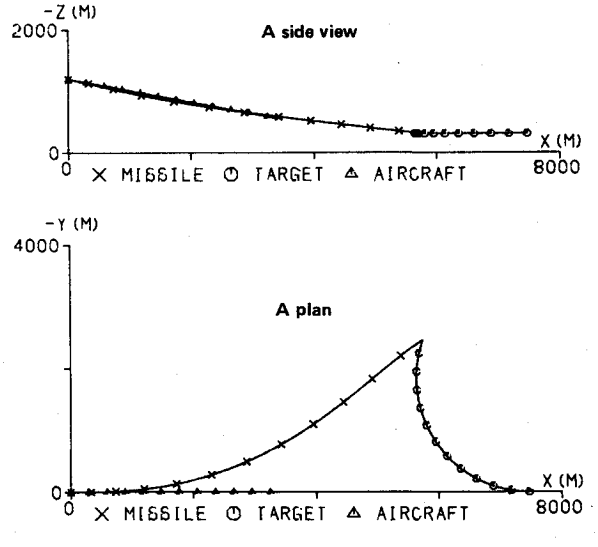

Fig. 5 Trajectories—look down case.

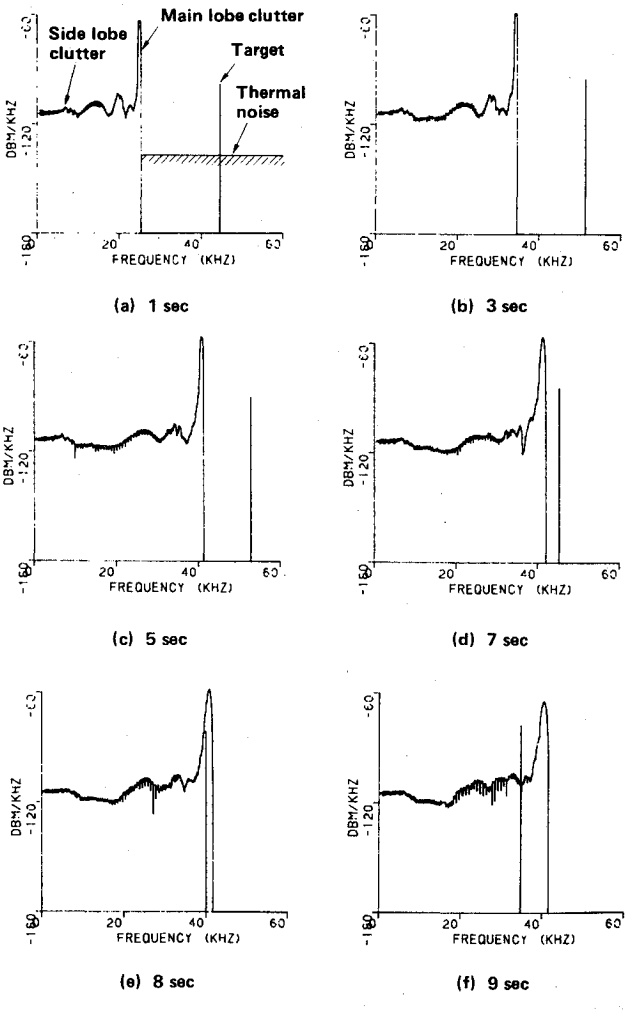

Fig. 6 Clutter spectra—look down case.

Table 1 Clutter in "equal altitude case"

Altitude, m	Main lobe, dBm/kHz	Side lobe, dBm/kHz
10000	−130	−130
6000	−113	−123
1200	−75	−117
300	−60	−113
100	−52	−110

Table 2 Clutter in "look up case"

Target altitude, m	Main lobe, dBm/kHz	Side lobe, dBm/kHz
3,600	−130	−120
1800	−120	−115
1200	−100	−110

Table 3 Main lobe clutter vs target in "spirally descending target case"

	Main lobe clutter		Target	
Time, s	Frequency, kHz	Level dBm/kHz	Frequency, kHz	Level, dBm/kHz
1	24	−102	44	−97
3	34	−96	49	−93
5	41	−70	46	−89
6	42	−65	42	−86
7	42	−65	36	−84

Spirally Descending Target Case

Finally,we assume that in the case where the target is at a higher altitude than the aircraft at the firing, a spirally descending maneuver is made. The aircraft at 1200 m aims at the predicted intercept point with the target at 1800 m. The target begins to turn to the lower altitude with 7 g lateral acceleration in the plane slanted by 35 deg off the horizontal plane, as soon as the missile is fired at a horizontal distance of 7000 m.

Table 3 shows the Doppler frequency and the level of the main lobe clutter and those of the target signal at various times. Although the main lobe clutter is lower at the beginning, it gradually develops until the target is completely covered at 6 s. This example shows that even a target at higher altitude will be masked by the main lobe clutter if it descends and turns properly.

From the foregoing cases, we can conclude that if the target flies below a cerain altitude, e.g. 300 m, there is a possibility for the missile to lose the target signal because of the main lobe clutter irrespective of the missile altitude.

Clutter Effects on a Missile Effective Zone

Preliminary Consideration

Consider how clutter status changes in relation to the missile initial position. For simplicity, the problem is handled in a horizontal plane as shown in Fig. 7. A target is located at the origin directing along the X axis and a missile is fired from any position aiming at a predicted intercept point. The transmitter is assumed to be located in the missile, and the aerodynamic limitations are not considered here.

At the initial moment, it is obvious that a missile fired from the right-hand side of the Y axis is in the clutter free (CF) zone, whereas one from the left-hand side of the Y axis is in the side lobe clutter (SC) zone. A missile on the Y axis, which flies in a narrow zone bordering the CF and SC zones is adversely affected by the main lobe clutter.

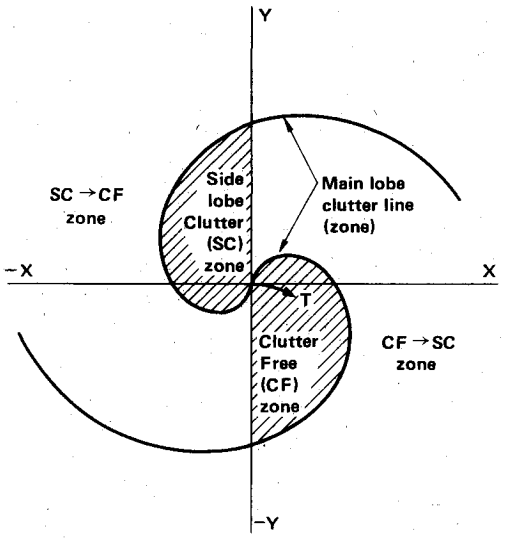

Fig. 7 Clutter status in relation to firing positions.

If the target flies straightforward, this situation is kept the same all through the missile flight time since the LOS does not rotate. If the target begins to turn clockwise as soon as the missile is fired, however, the clutter affected lines at the intercept time turn accordingly and are supposed to become spiral lines as shown in Fig. 7. These lines and the Y axis form a CF or SC zone. A missile fired in these zones can maintain CF or SC status throughout the flight. One fired outside these areas undergoes the change from CF to SC or vice versa. In other words, it must cross the main lobe clutter during the flight. One fired on the spiral line is adversely affected by the main lobe clutter at the terminal phase of the guidance.

Thus the influence of the main lobe clutter is categorized in two kinds. The first is the case where the missile crosses the main lobe clutter during the flight and the second is where the missile suffers the main lobe clutter at the terminal phase of the flight. The first problem may be solved by using a memory track and is not discussed here. A concept to avoid the second problem will be discussed later.

Simulation Results

Two cases of simulation are conducted to show the clutter influence on the missile effective zone. Parameters are described below where the target maneuvering conditions are selected referring to the aircraft data.[5]

Case 1:

Target $v_t = 350$ m/s, $a_t = 5\ g$, $h_t = 300$ m

Aircraft $v_a = 300$ m/s, $h_{a0} = 1200$ m

Case 2:

Target $v_t = 300$ m/s, $a_t = 7\ g$, $h_t = 300$ m

Aircraft same as Case 1

Figure 8 shows the horizontal projection of the simulation results. A target is located at the origin and directed along the X axis. An arrow represents the initial position and velocity vector of a missile which aims at the predicted intercept point. The target begins to maneuver clockwise at the time of the missile firing. Figures 8(a) and (b) correspond to case 1 and 2, respectively. The outer and inner contours show a missile effect zone limit calculated aerodynamically. The CF, SC, CF→SC, and SC→CF zones are ascertained as predicted in the preliminary consideration.

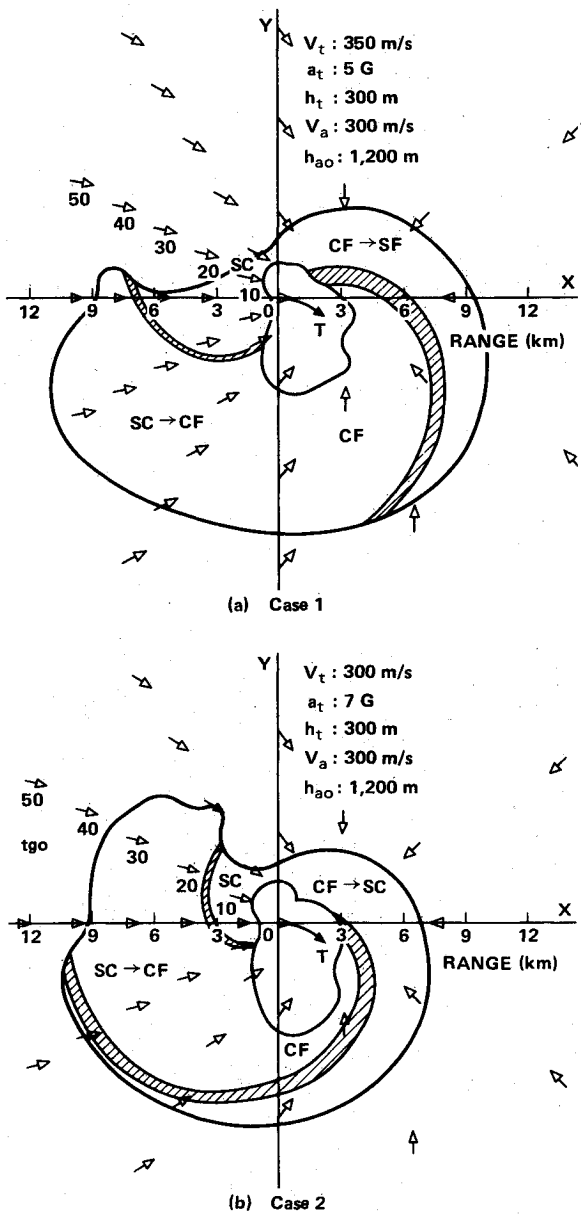

Fig. 8 Clutter effect on the missile effective zone.

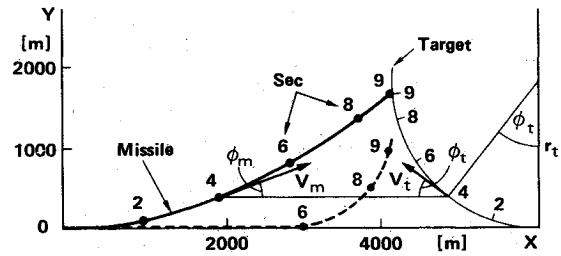

Fig. 9 Simplified trajectory analysis.

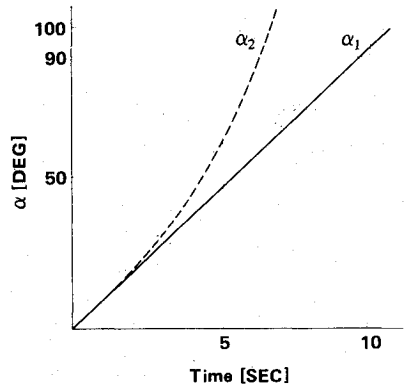

Fig. 10 Change of angle α with time.

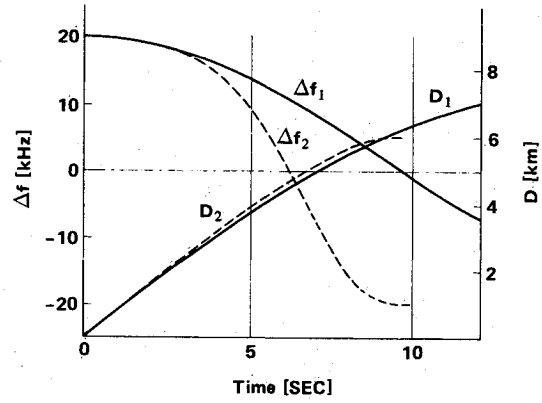

Fig. 11 Change of Δf and D with time.

The hatched portion between these contours shows the zones affected by the main lobe clutter. A missile fired from a point on the inner edge of the hatched zone begins to be adversely affected by the main lobe clutter at the intercept time. A missile fired from a point on the outer edge of the hatched zone suffers the main lobe clutter one second before interception and begins to recover from it at the intercept time. This means one second is assumed to be necessary for the missile to regain the normal guidance after its crossing over the main lobe clutter. The hatched portion is therefore the zone where the missile loses its effectiveness at the terminal guidance phase. It is seen that the missile is affected in the places where the maximum performance could be displayed if it were not for the main lobe clutter.

In case 1, the distance from the origin to the hatched zone is 5.6 km in pure initial head on (cross point with X axis), 10.2 km in 45 deg head on, 4.2 km in 45 deg tail chase, and 6.8 km in pure tail chase (cross point with $-X$ axis). In case 2, these values become 3.0 and 5.8 km in head on, and 1.8 and 3.2 km in tail chase, which are approximately one half of the values in case 1. This is caused by the target maneuvering condition difference.

A Suggestion to Avoid the Clutter Effect

The fact that a target maneuvering condition difference shifts the zones affected by the main lobe clutter indicates that a proper missile trajectory shaping would also shift them. It may be difficult for an analog type missile receiver to foretell when the main lobe clutter effect occurs. However, it would be easier for a digital type missile to memorize and forecast the target Doppler and the main lobe clutter movement and give a proper additional steering if necessary. The following discussion is based on this assumption.

Preliminary Analysis

Two trajectory examples are considered that show how the situation changes if the missile paths are different. Both the target and the missile are mass points and travel in a horizontal plane directly opposite at the initial time. The target with a speed of v_t begins to turn at the missile firing with a lateral acceleration of a_t. The radius of gyration r_t and the angular velocity Φ_t', are expressed by Eq. (5).

$$r_t = v_t^2/a_t, \qquad \Phi_t' = a_t/v_t \tag{5}$$

Example 1: It is assumed that the LOS does not rotate. Velocities of the target and missile have a relation expressed by Eq. (6). As α_1, the angle between LOS and $\mathbf{v}_t$ is equal to Φ_t. The frequency difference Δf_1, between the target Doppler and the main lobe clutter, is written by Eq. (7). The distance D_1, the sum of the distance the target and missile traveled along X axis, is calculated in Eq. (8).

$$v_t \sin\Phi_t = v_m \sin\Phi_m \tag{6}$$

$$\Delta f_1 = (2/\lambda) v_t \cos\Phi_t \tag{7}$$

$$D_1 = r_t \sin\Phi_t + \Sigma_{t=0}^{t} v_m \cos\Phi_m \Delta t \tag{8}$$

Parameters chosen here are: Initial distance = 6,000 m, $v_t = 300$ m/s, $a_t = 5$ g (giving $r_t = 1840$ m and $\Phi_t' = 9.4$ deg/s), $v_m = 500$ m, and $\Delta t = 0.5$ s. The trajectories for Example 1 are shown in Fig. 9, α_1 in Fig. 10, Δf_1 and D_1 in Fig. 11 with solid lines.

Example 2: In this example, the missile travels straightforward until t_2 s and turns with a lateral acceleration of a_m, after t_2 s. The angle α_2, the frequency difference Δf_2, and the distance D_2 in this example are obtained by Eqs. (9-11).

$$\alpha_2 = \Phi_t + \tan^{-1}\frac{r_t(1-\cos\Phi_t)}{R_{TM0} - v_m t - r_t \sin\Phi_t} \qquad \text{for } 0 \le t \sim t_2$$

$$= \Phi_t + \tan^{-1}\frac{r_t(1-\cos\Phi_t) - r_m\{1-\cos\Phi_m'(t-t_2)\}}{R_{TM0} - v_m t_2 - r_m \sin\Phi_m'(t-t_2) - r_r \sin\Phi_t} \qquad \text{for } t > t_2 \tag{9}$$

$$\Delta f_2 = (2/\lambda) v_t \cos\alpha_2 \tag{10}$$

$$D_2 = v_m t + r_t \sin\Phi_t \qquad \text{for } 0 \le t \le t_2$$

$$= v_m t_2 + r_m \sin\Phi_m'(t-t_2) + r_t \sin\Phi_t \qquad \text{for } t > t_2 \tag{11}$$

Additional parameters chosen here are: $a_m = 20$ G, (giving $r_m = 1300$ m and $\Phi_m' = 22.5$ deg/s) and $t_2 = 5$ s. The trajectories, α_2, Δf_2 and D_2 are shown in Figs. 9 through 11 with dotted lines.

In Example 1, the missile intercepts the target at 9.1 s, when the target is covered by the main lobe clutter since Δf_1 is almost zero. Whereas in Example 2, the missile is 500 m directly behind the target at 9.1 s and the target is already in the side lobe clutter since Δf_2 is -20 kHz.

Simulation Results

For verification a simulation is conducted for the case where a yaw fin bias command is added and compared with the normal proportional navigation. Conditions are same as the look down case of Fig. 5 with the exception of an initial range of 6000 m.

Figure 12 shows the results of the simulation only with horizontal projections. Figure 12a shows normal navigation with an intercept time of 8.76 s, if the missile does not suffer the main lobe clutter. Figure 12b shows a yaw fin deflection bias command by 30 deg is added between 2 and 6 s resulting in the intercept time of 9.28 s. The main lobe clutter and the target spectra are found to have the same Doppler frequency, between 7 and 7.8, s in both cases. This gives approximately 1 s allowance for the normal navigation case and 1.5 s for the fin deflection bias case, after passing through the main lobe clutter. The 0.5 s difference would favor the latter case.

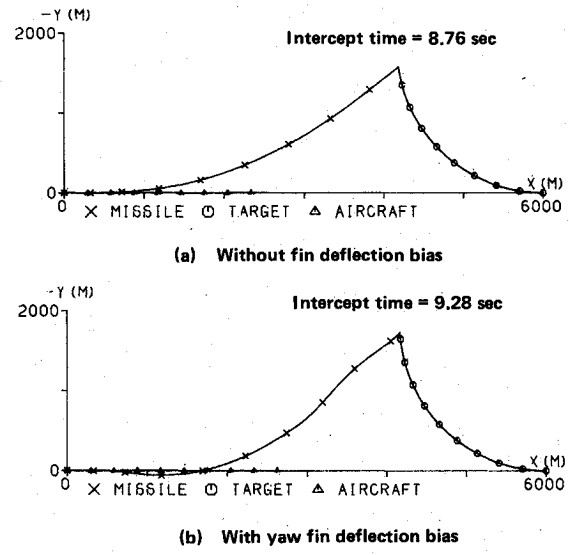

Fig. 12 Trajectories with and without fin deflection bias.

However, many kinds of algorithm may change the missile trajectory. More thorough investigation is required to establish the most effective method for this purpose.

Conclusions

A method combining the bistatic radar equation with the GPMS makes it possible to simulate clutter spectra in a semi-active radar homing missile at an arbitrary time interval. The clutter simulation reveals that if a target is below a certain altitude, e.g. 300 m, and turns with an appropriate lateral acceleration, the main lobe clutter masks the target signal.

Effective zone analyses of the missile are made by simulating two cases where $v_t = 350$ m/s, $a_t = 5$ g in case 1; and $v_t = 300$ m/s, $a_t = 7$ g in case 2. The results show that the missile aerodynamically effective zone is divided into the following zones from the clutter view point: CF, SC, CF→SC, SC→CF and main lobe clutter at the terminal phase. The last one, which is most critical for the missile, becomes spiral lines. These spiral lines change shape in cases 1 and 2, i.e., they cross X axis at 5.6 and -6.8 in case 1, and become 3.0 and -3.2 km in case 2. The missile trajectory shaping must be effective to avoid this main lobe clutter influence at the terminal phase. Applying fin deflection bias command is simulated as one of the countermeasures and has proved to be effective.

Acknowledgment

The authors are grateful to Dr. S. Uehara of Japan Defence Agency and to Prof. M. Higashiguchi of Tokyo University for their useful advice.

References

[1]Akishita, S. and Imado, F., "General Purpose Tactical Missile Simulation Program," *Proceedings of 13th Annual Simulation Symposium,* Society for Computer Simulation, Tampa, FL, 1980, pp. 257-270.

[2]Miwa, S. and Imado, F., "Calculation for the Clutter Spectrum in a Semi-Active Radar Homing Head," *Proceedings of ISNCR (International Symposium on Noise and Clutter Rejection),* IEEE and IECE, Tokyo, 1984, pp. 41-46.

[3]Skolnik, M.I., "Bistatic Radar," *Introduction to Radar Systems,* McGraw-Hill Book Co. 1980, p. 557.

[4]Skolnik, M.I., "Ground Echo," *Radar Handbook,* McGraw-Hill, 1970, pp. 25-26.

[5]Heffley, R.K. and Jewell, W.F., "Aircraft Handling Qualities Data," NASA CR-2144, 1972.